JOURNAL OF MATERIALS SCIENCE 17 (1982) 2486–2494

Microstructures and subcritical crack growth in oxidized hot-pressed Si_3N_4

G. DAS, M. G. MENDIRATTA, G. R. CORNISH
Systems Research Laboratories, Inc., 2800 Indian Ripple Road, Dayton, OH 45440-3696, USA

The microstructure of the oxide scales, primarily the size, distribution, and density of the pits, was characterized in hot-pressed Si_3N_4 oxidized at different temperatures from 1300 to 1450° C. These microstructural features and the chemical changes in Si_3N_4 due to oxidation were related to the elevated-temperature subcritical crack-growth (SCG) behaviour. Oxidation at 1375° C for 240 h resulted in a measurable improvement in SCG over that in as-hot-pressed and 1300° C-oxidized Si_3N_4.

1. Introduction

Many structural ceramics, e.g., hot-pressed (HP) Si_3N_4, SiC, and Al_2O_3, exhibit subcritical crack-growth (SCG) behaviour under load at elevated temperatures [1–5]. SCG can cause structural failure at a stress level significantly below the short-term fracture stress. The propagation of SCG is commonly related to the presence of glassy phases in the grain boundaries of these materials.

It has been observed [6, 7] that during oxidation of Si_3N_4 (hot pressed with MgO as a densification aid), Mg and Ca diffuse from the interior of Si_3N_4 to the external silica scale, creating an extensive depletion of Mg and Ca in the bulk. The removal of Mg and Ca which are the elements in the grain-boundary glassy phase reduces the viscosity of the glassy phase; therefore, after oxidation, the propensity for SCG should decrease. In fact, there is some evidence that the bulk creep resistance of HP-Si_3N_4 is improved through oxidation [8]. The present paper describes the microstructural observations of oxide layers resulting from oxidation of HP-Si_3N_4 at elevated temperatures and the effects of oxidation upon the subsequent SCG behaviour under the Mode I loading condition.

2. Experimental procedure

HP Si_3N_4 (NC–132) bend bars (5.08 cm × 0.640 cm × 0.32 cm) used in this study were purchased from Norton Co. For NC–132, MgO was used as a densification aid. The chemical analysis of Si_3N_4 is shown in Table I. The edges of the tensile surface of the bend bars were rounded to reduce edge flaws. The bend bars were polished on the tensile surface in a direction parallel to the specimen length on a 15 μm diamond wheel and then with 6 μm diamond paste prior to oxidation. Oxidation was carried out at 1300° C for 36 h, at 1375° C for 240 h and at 1450° C for 240 h inside the furnace in static air. Following oxidation, the oxide layer was removed in small steps from the tensile side by polishing with 6 μm diamond paste. After each step (removal of about 3 μm), the microstructure of the surface was examined by scanning-electron and light microscopy. Several controlled surface microcracks were produced on the tensile surface of the bend bars which had been carefully polished to remove the entire oxide layer. Nearly semicircular microcracks of an approximate radius of 90 μm were produced by a Knoop diamond indentor utilizing a 2.6 kg indentation load. The details of the technique involving the use

TABLE I Chemical analysis of NC–132 Si_3N_4

element	Mg	Al	Fe	Ca	Mn	B	W
content (wt %)	0.83	0.27	0.47	0.063	0.077	0.24	2

0022–2461/82/092486–09$03.58/0

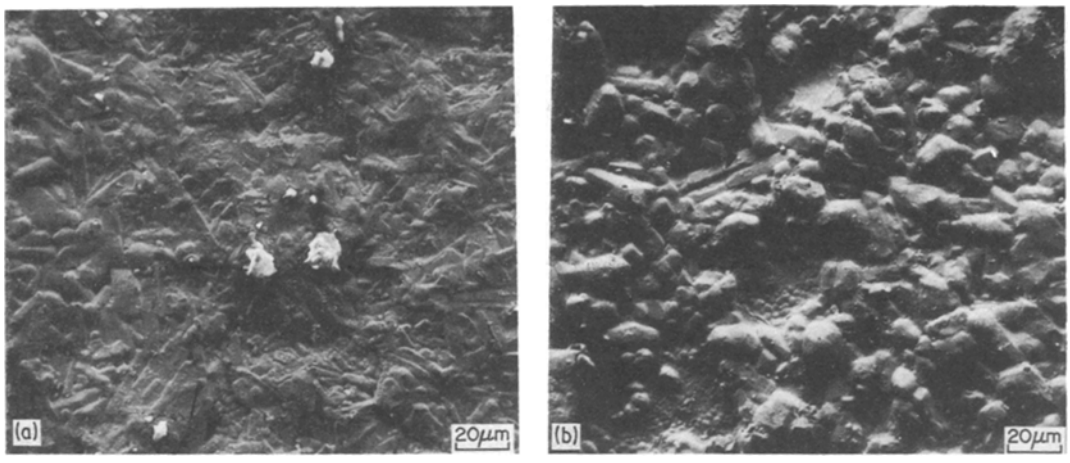

Figure 1 Scanning electron micrograph showing (a) both needle-like and gobular crystallites and (b) mainly gobular crystallites on the surface of HP-Si_3N_4 oxidized at 1300° C for 36 h.

of controlled flaws in studying the SCG of HP-Si_3N_4 have been described in a recent publication [9].

The bend bars containing the controlled cracks were subjected to a predetermined stress of 196 MN m^{-2} (28.5 x 10^3 psi) in a four-point-bend fixture on an Instron at 1300° C in a vacuum of ~ 10^{-5} Torr for various hold times in order to grow the cracks subcritically. It has been shown [9] that significant SCG occurs at the stress and temperature values selected for the present study. The applied stresss was perpendicular to the crack plane, creating a Mode I loading condition. The predetermined stress was reached using a cross-head speed of 5 x 10^{-3} cm min^{-1}; once the desired stress was attained, the cross-head movement was stopped. In most of the experiments, the stress was held at the desired level by manual control until fracture. The surface-crack extensions were measured by light and scanning-electron microscopy. Average crack-growth velocity was calculated by dividing the crack extension by the corresponding hold time.

3. Results

3.1. Microstructures of as-oxidized surface layers

The surface oxide layer in HP-Si_3N_4 resulting from oxidation at 1300° C for 36 h consists of needle-like and globular crystallites as shown in Fig. 1. Cracks were readily visible in the oxide layers (shown by arrows in Fig . 1). The thickness of the oxide layer as determined from a cross-sectional view was rather non-uniform throughout. An average thickness was determined to be about 12 μm. Occasional large pits were observed within the oxide layer (Fig. 2).

The oxide-scale morphology in Si_3N_4 following oxidation at 1375° C for 240 h is shown in Fig. 3 to consist of well-developed needle-like crystallites with cracks being present. The thickness of the oxide layer was found to vary throughout the cross-section, and an average thickness was determined to be about 50 μm.

A significant change in the appearance of the oxide-scale morphology occurred after oxidation at 1450° C for 240 h. The oxide surface layer appeared glassy and was highly non-uniform with readily observable cracks, as shown in Fig. 4. Visual inspection revealed a glazed appearance

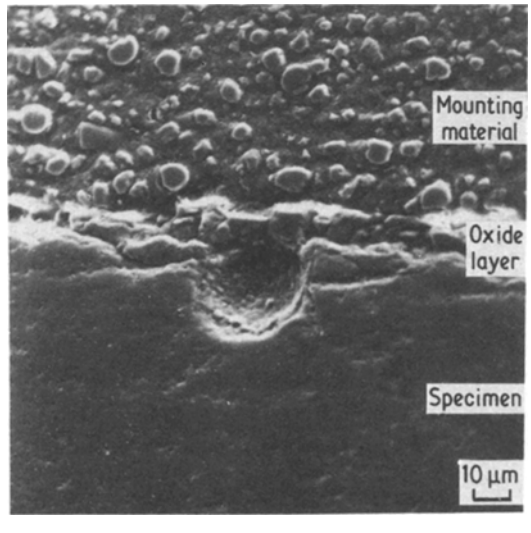

Figure 2 Scanning electron micrograph showing a large pit in the oxidized layer (cross-sectional view) of HP-Si_3N_4 oxidized at 1300° C for 36 h.

Figure 3 Scanning electron micrograph of the surface of HP-Si_3N_4 oxidized at 1375° C for 240 h.

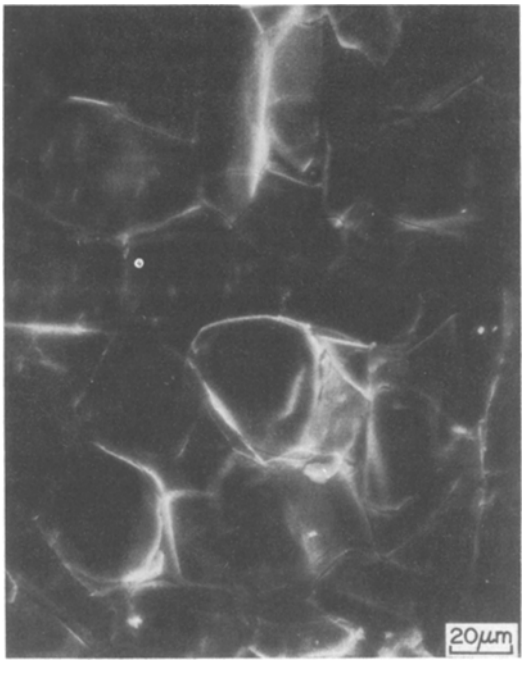

Figure 4 Scanning electron micrograph of the surface of HP-Si_3N_4 oxidized at 1450° C for 240 h. Cracks are readily observed.

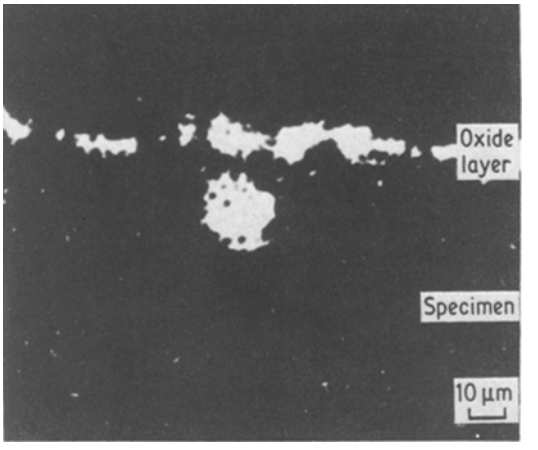

Figure 5 Electron-microprobe scan showing Ca concentration mostly at the outer oxide layer (light areas) in HP-Si_3N_4 oxidized at 1300° C for 36 h (cross-sectional view).

in some regions, suggesting that melting of the oxidized layer had occurred during oxidation. Tripp and Graham [10] made a similar observation in their oxidation of Si_3N_4 at 1450° C. In the present experiments, sagging in the middle of the bars was visible after oxidation at 1450° C for 240 h. Although sagging was also observed after oxidation at 1300 and 1375° C, the relative magnitude is very small compared to that observed for bars oxidized at 1450° C. Oxidation at 1450° C for 240 h resulted in a considerably thicker oxide scale, with large variation throughout the cross-section, ranging from 25 to 250 μm.

Electron-microprobe and energy dispersive X-ray analysis (EDAX) examinations were performed on oxidized specimens to determine qualitatively the chemical concentration, especially of Mg and Ca, within the oxidized scale. Electron-microprobe analysis of a cross-section of a specimen oxidized at 1300° C for 36 h showed that the concentration of Mg was high in the outer oxide layer and decreased to a constant level at a distance of approximately 100 to 150 μm from the outer oxide layer. The Ca concentration was very low in the specimen, but a concentration of Ca-rich material was detected in the outer oxide layer (see Fig. 5). Qualitatively, similar observations were made for specimens oxidized at 1375° C for 240 h and 1450° C for 240 h. These observations are in agreement with earlier investigations [7].

EDAX also showed the outer oxidized surface to be rich in Mg and Ca in all oxidized specimens.

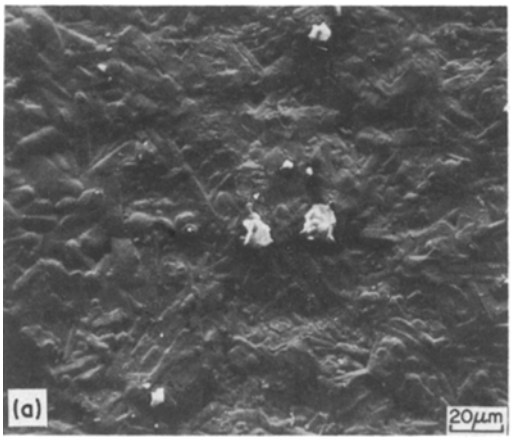

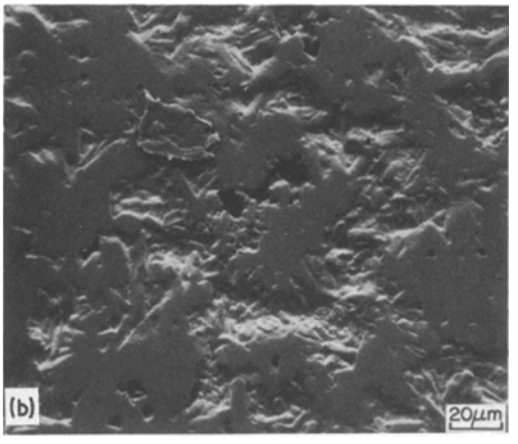

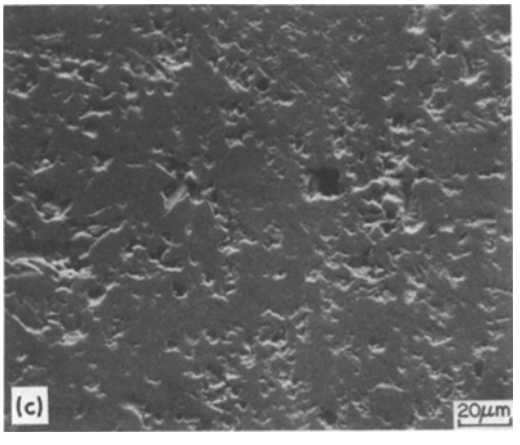

Figure 6 Progressive removal of outer oxidized layer in Si_3N_4 oxidized at 1300° C and for 36 h (same are) showing (a) As oxidized layer, (b) 15 μm removed and (c) 22.5 μm removed.

In addition, small WC particles (presumably introduced during the ball-milling operation) were present in both as-hot-pressed and-oxidized Si_3N_4 .

Prior to introduction of the controlled cracks in the oxidized bars, the oxide layer was removed by polishing with 6 μm diamond paste. Figs 6 to 8 show the microstructures corresponding to the progressive removal of the oxide layers of Si_3N_4 oxidized at 1300° C for 36 h, 1375° C for 240 h, and 1450° C for 240 h, respectively. Pits become visible as material is gradually removed from the oxidized layers. These pits are thought to be due to gaseous evolution and entrapment (N_2 and/or SiO) as a result of the oxidation reaction and have been reported in many previous investigations on HP-Si_3N_4 [10, 11]. Numerous pits of different sizes are observed in 1300° C-oxidized Si_3N_4 even after the oxidized layer has been completely removed (Fig. 6c). The pit-size distribution in the surface following removal of the oxide layers in 1300° C-oxidized Si_3N_4 is shown in Fig. 9. In general, the population density of pits having dimensions of 5 μm of less was the highest, followed by pits having sizes between 5 and 10 μm. The number of pits having dimensions greater than 10 μm was low, and only a few pits having dimensions greater than 20 μm were observed. On the other hand, pits remaining on the surface after the oxide layer had been removed in 1375° C-oxidized specimens appeared to have a more or less uniform distribution (Fig. 7). Most of them were spherical in shape with an average size of 40 μm. In contrast, the size of the pits observed on the surface following removal of the oxide layer in 1450° C-oxidized specimens was very small compared to those in 1300- and 1376° C-oxidized specimens; however, their density was significantly higher. Occasionally, large pits were also present in the oxide scale (Fig. 8).

3.2. Subcritical crack growth

3.2.1. As-hot-pressed Si_3N_4

As-hot-pressed Si_3N_4 bars having controlled flaws on the tensile surface were subjected to a stress of 196 MN m^{-2} (28.5 x 10^3 psi) at 1300° C in four-point-bend tests until fracture occurred. It has been observed that time-to-fracture varied from 7 to 17 min. In all cases, fracture took place away from the controlled flaws at the cracks growing subcritically from the edge of the sample.

SCG from the controlled flaws was observed in all of the above specimens, as shown in Fig. 10. The controlled flaws grew along the initial plane

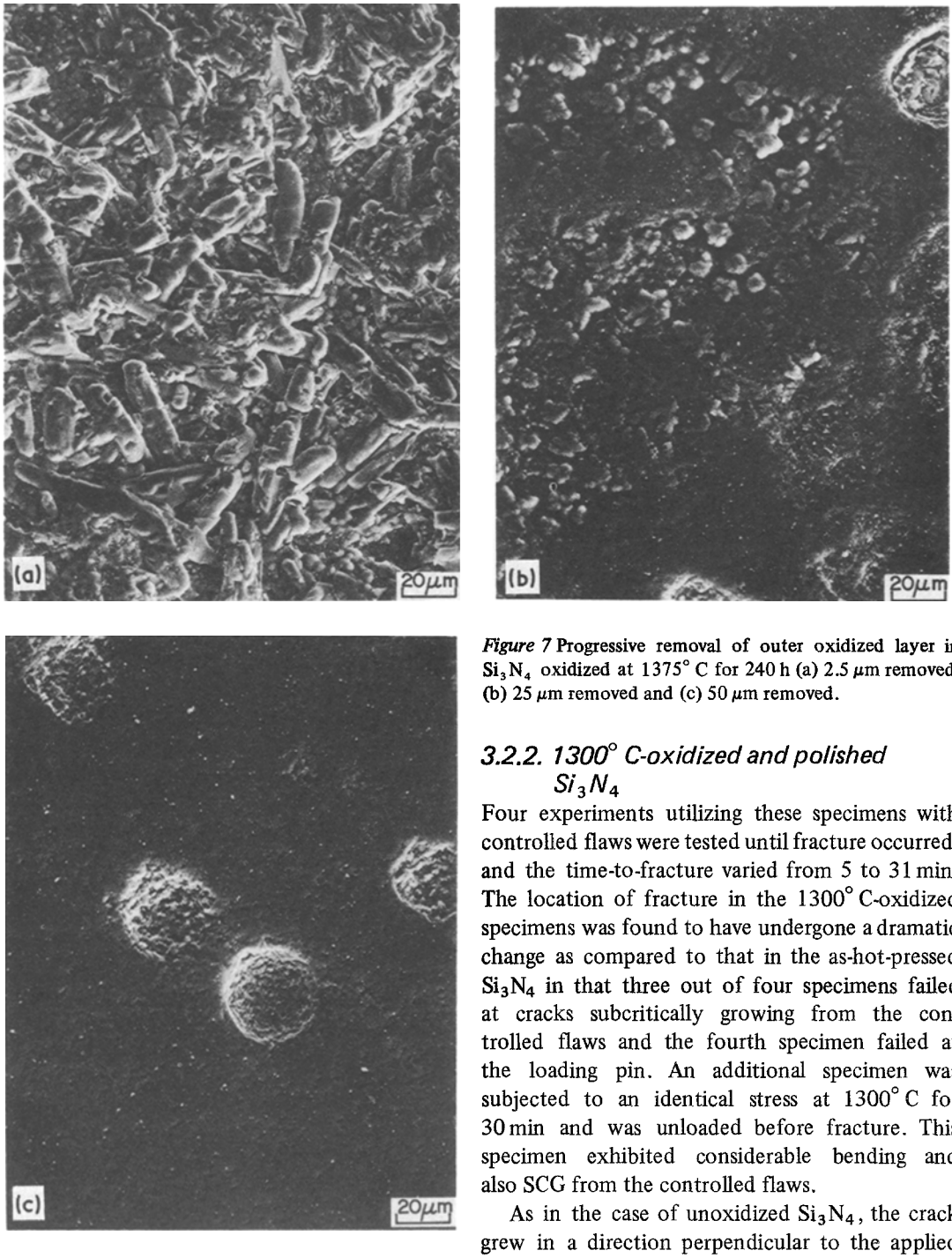

Figure 7 Progressive removal of outer oxidized layer in Si_3N_4 oxidized at 1375° C for 240 h (a) 2.5 μm removed, (b) 25 μm removed and (c) 50 μm removed.

of the indent in a direction perpendicular to the applied load. Crack extension was observed at both ends of the initial indent, the amount of extension being approximately the same. The crack path was rather straight, with some crack branching.

3.2.2. 1300° C-oxidized and polished Si_3N_4

Four experiments utilizing these specimens with controlled flaws were tested until fracture occurred, and the time-to-fracture varied from 5 to 31 min. The location of fracture in the 1300° C-oxidized specimens was found to have undergone a dramatic change as compared to that in the as-hot-pressed Si_3N_4 in that three out of four specimens failed at cracks subcritically growing from the controlled flaws and the fourth specimen failed at the loading pin. An additional specimen was subjected to an identical stress at 1300° C for 30 min and was unloaded before fracture. This specimen exhibited considerable bending and also SCG from the controlled flaws.

As in the case of unoxidized Si_3N_4, the crack grew in a direction perpendicular to the applied load (Fig. 11); however, it deviated from the initial plane of the indent, and the amount of crack extension at each end of the initial indent was different. Considerable crack branching was observed together with cracks emanating from the natural flaws. Frequently, the crack growing from the initial indent was found to disappear at one end of a pit present in the oxidized and

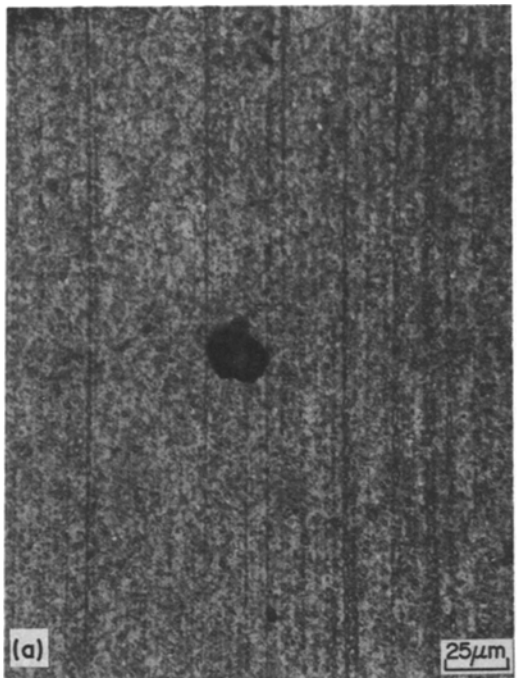

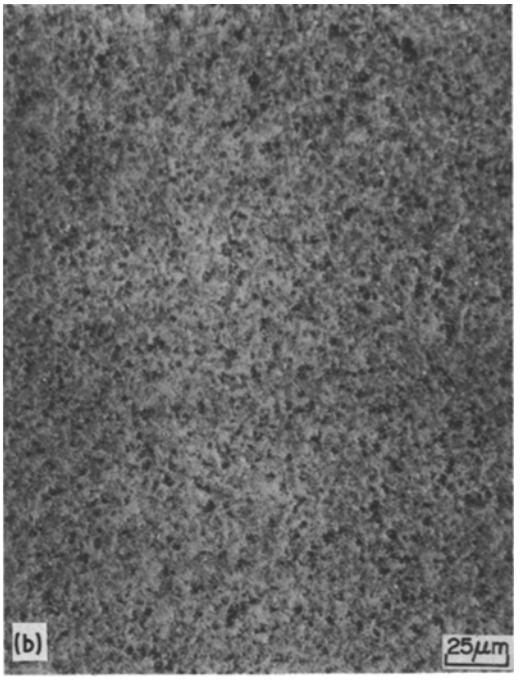

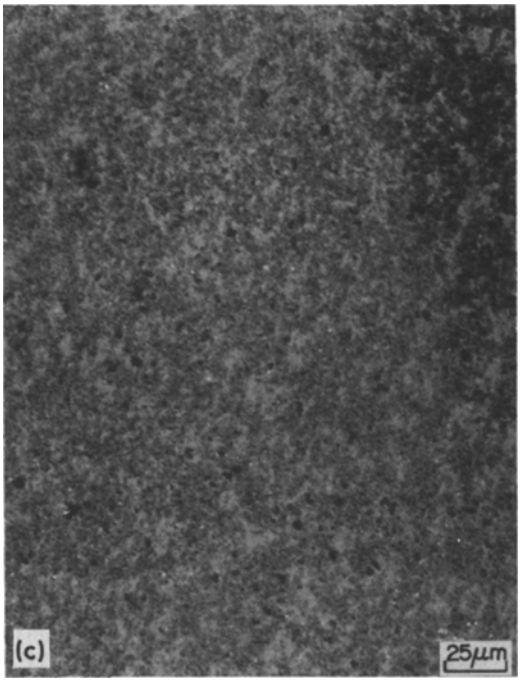

Figure 8 Progressive removal of outer oxidized layer in Si_3N_4 oxidized at 1450° C for 240 h (a) 12 μm removed, (b) 25 μm removed and (c) 50 μm removed.

polished material and to become visible again at the other end. In addition, a number of cracks from pits was also observed.

3.2.3. 1375° C-oxidized and polished Si_3N_4

The time required to fracture was higher for 1375° C-oxidized bars than that for as-hot-pressed and 1300° C-oxidized specimens. It varied from 31.5 to 47 min. All three bars failed from cracks subcritically growing from the controlled flaws. Additionally, the slow-crack-growth behaviour was essentially the same as described earlier.

3.2.4. 1450° C-oxidized and polished Si_3N_4

These specimens failed at 117 and 172 MN m^{-2} before attaining the predetermined stress level of 196 MN m^{-2} when tested in four-point bending at 1300° C. However, no evidence for cracks growing subcritically from the controlled flaws was found. It may be speculated that the high density of small pits and occasionally large pits present in the specimen following oxidation at 1450° C act as stress-raisers and lead to catastrophic failure long before the controlled cracks become critical.

Data on time to fracture for as-hot-pressed and oxidized bend bars subjected to a stress of 196 MN m^{-2} (28.5 x 10^3 psi) at 1300° C for different oxidation treatments are plotted in Fig. 12. It appears that oxidation of Si_3N_4 at 1375° C for 240 h has led to an improvement over that of the as-hot-pressed and 1300° C-oxidized speci-

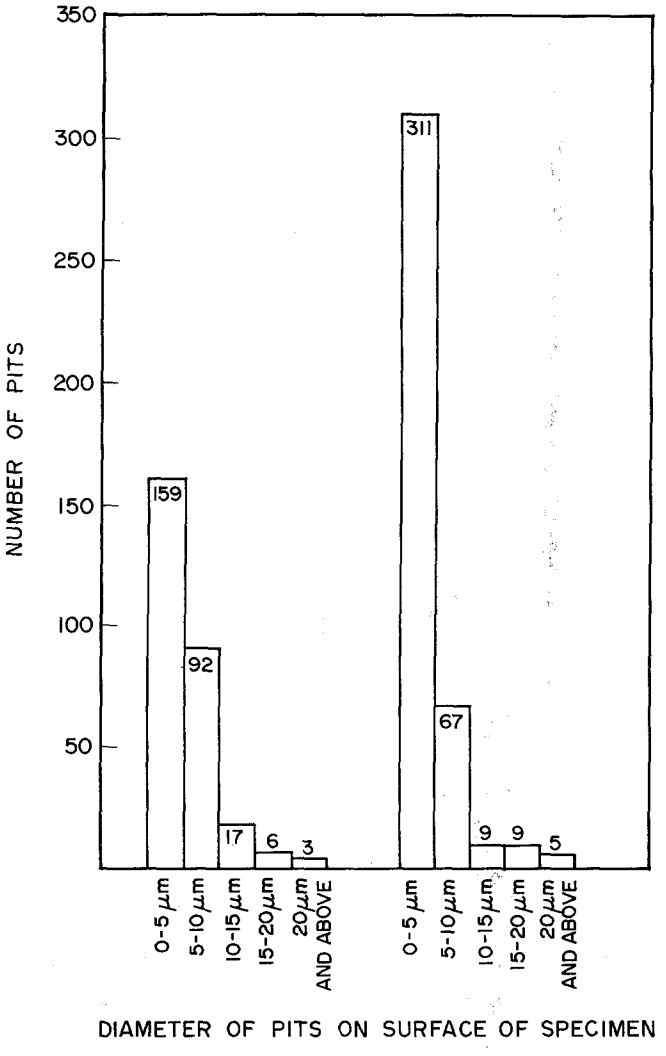

Figure 9 Pit-size distribution in specimens following removal of oxidized layer in Si_3N_4 oxidized at 1300° C for 36 h. Total area observed is approximately 200 μm × 180 μm in each case.

mens with regard to retarding slow-crack-growth behavour.

4. Discussion

Several factors are known to affect SCG behaviour in Si_3N_4, including (a) the chemical nature of the grain-boundary glass phase, (b) microstructural inhomogeneities, (c) chemical inhomogeneities, and (d) surface conditions. From the microprobe results, it is evident that Mg and Ca have diffused from the interior of the oxidized Si_3N_4 to the external oxidized surface. Mg and Ca are the elements in the grain-boundary glassy phase which reduce viscosity at high temperature, and the propensity for SCG should decrease after oxidation. The explanation is based upon the

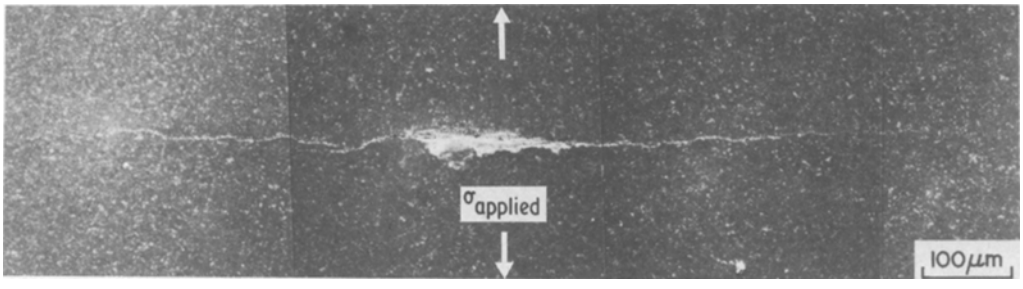

Figure 10 Crack extension in as-received Si_3N_4 tested in four-point bending at 1300° C. Applied stress is 196 MN m^{-2}.

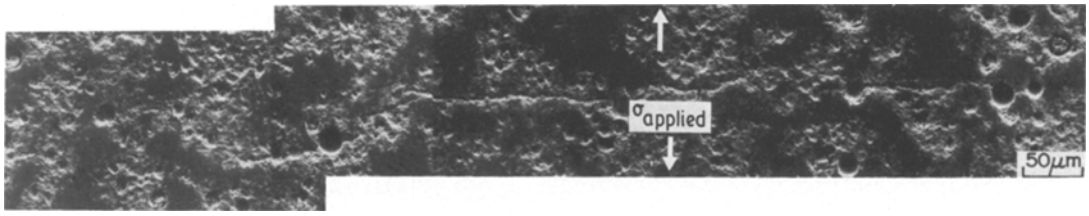

Figure 11 Crack extension in 1300° C-oxidized Si_3N_4 tested in four-point bending at 1300° C. Applied stress is 196 MN m^{-2}.

assumption that the micromechanism of SCG involves localization of the bulk-creep process ahead of the main crack. Due to stress intensification at the tip of the controlled flaw, creep occurs at a stress higher than that experienced by the bulk specimen. It has been suggested that in the high stress range (150 to 350 MN m^{-2}), the creep process in HP-Si_3N_4 is controlled by the rate of relative movement of grains caused by grain-boundary sliding and microcracking [12]. Thus, any treatment which decreases grain-boundary sliding (e.g., reduction of the viscosity of the grain-boundary phase) will result in the reduction of SCG. It has also been shown that the bulk creep resistance of HP-Si_3N_4 was improved through oxidation [8]. In hot-pressed β' Si–Al–O–N ceramics, high-temperature (diffusional) creep and SCG properties were also improved by elevated-temperature heat treatments [13].

It has been observed that in as-hot-pressed Si_3N_4 with controlled flaws subjected to four-point-bend tests at 1300° C, fracture always takes place from flaws subcritically growing from the edge. This seems to suggest that chemical and microstructural inhomogneities in this material are so severe that due to the occurrence of extensive creep, natural flaws readily become critical before the controlled flaws. However, upon oxidation at 1300° C, the majority of bars failed from cracks growing from the controlled flaws. This situation was further improved upon oxidation at 1375° C when all bend bars failed from cracks growing from the controlled flaws, although cracks growing from natural flaws were also observed. This behaviour, coupled with the observations that bend bars oxidized at 1375° C for 240 h yielded longer hold times to fracture as compared to those of as-hot-pressed and 1300° C-oxidized specimens, suggests that oxidation at elevated temperatures must result in a modification of the chemical and microstructural heterogeneity in the Si_3N_4 in such a way that the controlled flaws become critical before other natural flaws have the opportunity to do so.

It should be mentioned, however, that although an overall improvement in the SCG behaviour was

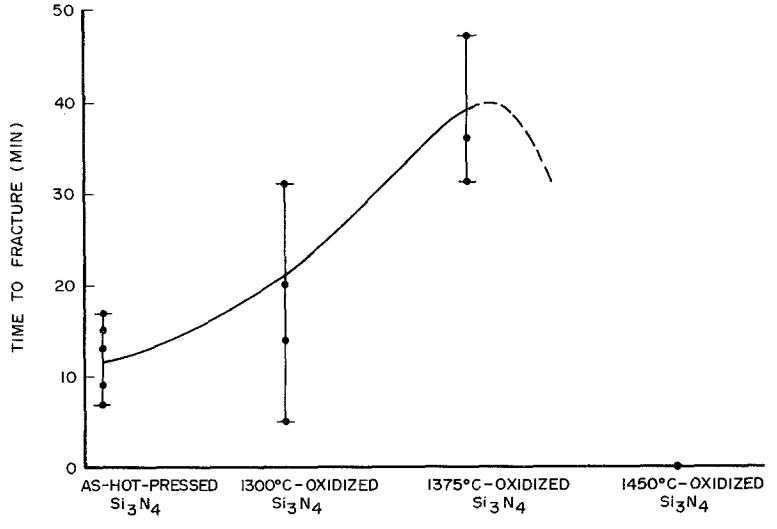

Figure 12 Hold time to fracture for as-hot-pressed, 1300° C-oxidized, and 1375° C-oxidized Si_3N_4 tested in four-point bending at 1300° C. Applied stress is 196 MN m^{-2}.

achieved in 1375° C-oxidized Si_3N_4 despite the presence of pits (average size of about 40 μm), the beneficial effects of oxidation upon the SCG behaviour cannot be fully realized unless the formation of pits which results from oxidation at elevated temperatures can be eliminated or minimized.

5. Summary and conclusions

The surface oxide layer in HP-Si_3N_4 resulting from oxidation at 1300 and 1375° C in static air consisted of needle-like and globular crystallites. The oxide layer appeared to have undergone melting at 1450° C. Cracks were observed in the surface oxide layers of all specimens.

Pits present in the surface following removal of the oxide layer showed a variation in size, with the density of pits having dimensions of 5 μm or less being the highest at 1300° C. At 1375° C, pits were more or less spherical with an average size of 40 μm. On the other hand, numerous small pits were observed at 1450° C.

Oxidation at 1375° C resulted in a measurable improvement in SCG over that of as-hot-pressed and 1300° C-oxidized Si_3N_4, despite the presence of pits. However, it is believed that the beneficial effects of oxidation upon the SCG behaviour cannot be fully realized unless the formation of pits can be eliminated or minimized.

Acknowledgements

The authors wish to thank B. M. Lipsitt for experimental assistance. This program was supported by U. S. AFOSR Contract F49620-77-C-0124.

References

1. F. F. LANG, *J. Amer. Ceram. Soc.* **57** (1974) 84.
2. A. G. EVANS and S. M. WIEDERHORN, *J. Mater. Sci.* **9** (1974) 270.
3. A. G. EVANS, M. LINZER and L. R. RUSSELL, *Mater. Sci. Eng.* **15** (1974) 253.
4. A. G. EVANS, in "Ceramics for High Performance Applications", Proceedings of the Second Army Materials Technology Conference, Hyannis, Massachusetts, 13 to 16 November 1973, edited by J. J. Burke, A. E. Gorum and R. N. Kate (Brook Hill Publishing Co., Chestnut Hill, MA, 1974) p. 373.
5. K. D. MCHENRY and R. E. TRESSLER, *J. Amer. Ceram. Soc.* **63** (1980) 152.
6. S. C. SINGHAL, *J. Mater. Sci.* **11** (1976) 500.
7. D. CUBICCIOYTI, K. H. LAU and R. L. JONES, *J. Electrochem. Soc.* **124** (1977) 1955.
8. F. F. LANGE and B. I. DAVIS, *Bull. Amer. Ceram. Soc.* **59** (1980) 827.
9. M. G. MEDNIRATTA and J. J. PETROVIC, *J. Amer. Ceram. Soc.* **61** (1978) 226.
10. W. C. TRIPP and H. C. GRAHAM, *ibid.* **59** (1976) 399.
11. A. J. KIEHLE, L. K. HEUNG, P. J. GIELISSE and T. J. ROCKETT, *ibid.* **58** (1975) 17.
12. J. M. BIRCH and B. WILSHIRE, *J. Mater. Sci.* **13** (1978) 2927.
13. B. S. B. KARUNATATNE and M. H. LEWIS, *ibid.* **15** (1980) 1781.

Received 15 June 1981
and accepted 26 January 1982